Uplift of model steel pipelines embedded in polycrystalline ice
Rajani, B. B.; Morgenstern, N. R.

This publication could be one of several versions: author's original, accepted manuscript or the publisher's version. / La version de cette publication peut être l'une des suivantes : la version prépublication de l'auteur, la version acceptée du manuscrit ou la version de l'éditeur.

National Research Council Canada   Conseil national de recherches Canada

Canada

NRC · CNRC

Uplift of model steel pipelines embedded in polycrystalline ice

B. RAJANI AND N. MORGENSTERN

(NRCC-38461)(IRC-p-3860)

Canadä

13780235

Uplift of model steel pipelines embedded in polycrystalline ice

B. Rajani[1] and N. Morgenstern

University of Alberta, Department of Civil Engineering, Edmonton, Alta., Canada T6G 2G7

The experimental behaviour of model pipelines embedded in polycrystalline ice is studied to improve the understanding of the behaviour of a chilled buried pipeline subjected to frost heave. Two model pipelines with slightly different radius to thickness ratios were subjected to prescribed displacement rates. Their behaviour was monitored until peak strains corresponding to current acceptable strain limits, often referred to as the wrinkling strains, were exceeded. The sizing of the model pipelines and experimental setup are described and detailed procedures on polycrystalline ice sample preparation are given. Representative core samples of polycrystalline ice were tested to determine its elastic and creep properties. The observed and predicted responses of strain histories in the pipeline are compared and acceptable agreement between the responses is obtained.

Key words: experimental behaviour, embedded model pipelines, polycrystalline ice, frost heave, uplift resistance, critical strain limits.

Le comportement expérimental de pipelines modèles enfouis dans la glace polycristalline est étudié de façon à améliorer la compréhension du comportement d'un pipeline froid enfoui subissant un soulèvement dû au gel. Deux pipelines modèles ayant des rapports rayons sur épaisseur légèrement différents ont été soumis à des vitesses de déplacement données. Leur comportement a été mesuré jusqu'au dépassement des déformations de pic correspondant à des limites de déformation couramment acceptées, souvent appelées déformations de plissement Le dimensionnement des pipelines modèles et le montage expérimental sont décrits, et les procédures détaillées pour la préparation des échantillons de glace polycristalline sont données. Des carottes représentatives de glace polycristaline ont été soumises à des essais pour déterminer ses propriétés élastiques de même que ses propriétés de fluage. Les réactions observées et prédites des histoires de contrainte dans le pipeline sont comparées, et une concordance acceptable entre les réactions est obtenue.

Mots clés : comportement expérimental, pipelines modèles enfouis, glace polycristalline, soulèvement dû au gel, résistance au soulèvement, limites de déformation critique.

[Traduit par la rédaction]

Introduction

Over the past decade several proposals have been put forward for the construction of a gas pipeline from the Arctic to the southern populated areas of North America (American Society of Civil Engineers 1978). These pipelines must be buried because of regulatory requirements that are intended to minimize environmental damage. It has been suggested that by transporting gas at below-freezing temperatures (i.e., chilled gas) the thawing of permafrost soils would be avoided. The transmission of chilled gas would lead to freezing of unfrozen soils in zones of shallow and discontinuous permafrost. A frozen annulus will develop in a frost-susceptible soil around the gas pipeline, leading to significant water migration to the freezing front and the formation of ice lenses. Consequently, the induced frost heave will force the pipeline to move upwards. The pipeline will undergo substantial straining which can lead to the formation of wrinkling buckles, especially when the pipeline traverses a transition zone between two soils with different frost susceptibilities or between an unfrozen and previously frozen soil. Ever since the chilled gas pipeline concept was proposed, the effect of frost heave on the performance of pipelines was identified as an important issue that should be addressed. A designer would have to

determine the level of strains that can be tolerated in a pipeline before serviceability is seriously hindered and ultimately if structural integrity is to be assured.

To date, only one experimental pipeline facility has been set up (Caen, France) that attempts to monitor the development of strains in the pipeline as differential frost heave develops. A lot of economical and experimental effort has been devoted to obtain this unique set of data, and indeed the data can be very useful in the validation of models on frost heave, frozen soil – pipeline interaction, etc. The details of the experimental data are available through numerous reports (Dallimore and Crawford 1985; Geotechnical Sciences Laboratories 1986, 1988, 1989).

The pipeline (0.273×0.0048 m) tested at Caen never experienced strains beyond the elastic strain limit. The pipeline underwent four freeze–thaw cycles and, since the response of the pipeline during each cycle was slightly different, the interpretation of the responses led us to infer that factors such as homogeneity of creep soil properties need to be addressed as discussed previously (Rajani 1992). A major source of uncertainty in the field experimental studies, as in those performed at Caen, is in the geomechanical (both elastic and creep) properties. As indicated by Rajani and Morgenstern (1992), the elastic and creep properties are crucial to the reliable prediction of stresses in the pipeline. The elastic moduli obtained from test samples on sand and silt were unusually high, as discussed by Rajani (1992). In addition, the reported

TABLE 1. Comparison of characteristics of pipeline at Caen, France, and model pipelines

Parameter	Pipeline at Caen	Model A	Model B
Pipeline structural characteristics			
Pipeline diameter D (m)	0.273	0.0381 (1.5 in.)	0.0508 (2 in.)
Pipeline thickness t (mm)	4.8	0.889 (0.035 in.)	1.245 (0.049 in.)
Pipeline material	Steel	Stainless steel 304	Stainless steel 304
R/t pipeline ratio	28.44	21.43	20.40
Elastic modulus E (GPa)	210	193	193
Poisson's ratio ν	0.3	0.3	0.3
Yield strength σ_y (MPa)	240	193	193
Bin size			
Half width (m)	9.0 (33D)	1.6 (42D)	1.6 (31D)
Width (m)	8.0 (29D)	0.6 (16D)	0.6 (12D)
Height (m)	1.7 (6D)	0.4 (10D)	0.4 (8D)
Embedment h (m)	0.33 (1.2D)	0.04 (1.05D)	0.06 (1.18D)
Soil–ice characteristics			
Elastic modulus E_s (MPa)	2.82, sand; 0.96, silt	3–7 GPa	3–7 GPa
Dry density γ (kN/m^3)	18.52, sand; 16.29, silt	8.54	8.46
Void ratio e	0.40–0.44, sand; 0.59–0.63, silt	0.06	0.07–0.08
Poisson's ratio ν_s	0.3	0.32	0.34
Creeping material	Sand/silt	Ice	Ice
Creeping exponent n	5.6/10.6	2.84	2.84

creep exponent n in the Norton creep flow law for silt is presumed to be on the high side. Small-scale laboratory model testing, where careful control can be exercised over the different aspects of the frozen soil – pipeline interaction, is warranted, and the results would serve to complement some of the observations at the Caen experimental facility. It would also lead to a better understanding of the frozen soil – pipeline interaction problem. Polycrystalline ice is the preferable medium for embedment, since its elastic and creep properties have been confirmed through a considerable amount of testing by different researchers. These tests are also intended to validate findings of Rajani and Morgenstern (1992) on the behaviour of an embedded beam in a creeping medium. The use of polycrystalline ice reduces the uncertainties in the experimental results, so the differences in the theoretical predictions and experimental observations cannot be solely attributed to variations in properties of the surrounding frozen medium. Nonetheless, typical data (Table 1) on mechanical properties of polycrystalline ice and frozen soil indicate that there is not much qualitative difference in the elastic and creep behaviour between the two material types. Another objective of carrying out these tests was to develop sufficient resistance to uplift in the model pipelines so that portions of the pipeline would strain beyond the elastic limit and well beyond the currently accepted strain limits. These arguments provided a basis for carrying out scaled laboratory testing of model pipelines in polycrystalline ice.

Nixon (1984) performed experiments on solid model piles embedded in polycrystalline ice, but several aspects such as shallow embedment, imposed displacements or the implications of a thin tubular section (i.e., radius thickness ratio) were not addressed. More recently, Foriero and Ladanyi (1991) have performed lateral load tests on aluminum (tubular) and steel (solid) model piles embedded in frozen sand, but again aspects of particular interest to pipelines were not studied. These aspects would not normally be of major concern for the design of laterally loaded piles.

In a realistic scenario, frost penetration would proceed on the commencement of transportation of chilled gas, and frost heave in the frost-susceptible soil would develop concurrently. The testing of a model pipeline embedded in polycrystalline ice assumes that the freezing of the surrounding soil in the field takes place instantaneously. In practice the pipeline would interact with increasing extent of frozen soil as the frost front advances. It is expected that significant uplift resistance develops within the frozen soil mass immediately above and around the chilled gas pipeline. The fact that the stress wave in the pipeline at Caen formed during the early stages of the experiment and that its shape did not change significantly with time supports this view.

Equipment design

The experimental setup to study pipeline – polycrystalline ice interaction involves three basic aspects: (*i*) the proportioning of the model pipelines and of the surrounding polycrystalline ice sample, (*ii*) the preparation of the ice block sample itself, and (*iii*) the loading arrangement that adequately represents frost heave. Each of these aspects will be described in detail, followed by experimental observations of the model pipelines subjected to an end prescribed displacement rate.
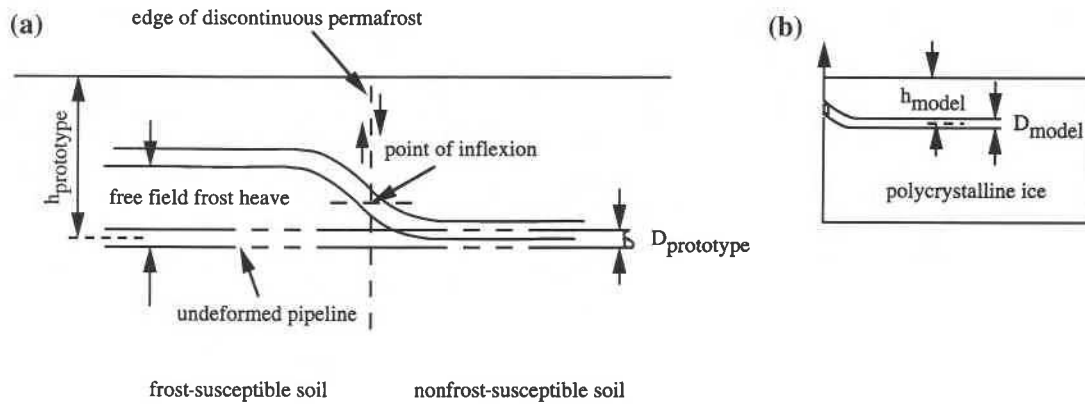
FIG. 1. Comparison of (a) prototype in field conditions and (b) experimental model (not to scale).

A prototype pipeline crossing the zone of discontinuous permafrost would be subjected to high strains in that portion of the pipeline embedded in a previously unfrozen soil. The response of the pipeline subjected to a steady frost heave at the interface of the discontinuous permafrost would have nearly double curvature if the stiffness of the frozen soil were quite high. The experience at the Caen experimental facility (Dallimore and Crawford 1985) indicates that the nearly double curvature response exists despite the relatively shallow burial of the pipeline. The plane strain study, performed by Nixon et al. (1983) of a continuum where one half of the soil was frost susceptible and the pipeline was considered to be passive, indicated that the response had double curvature. These considerations indicate that it would suffice to model only one half of the pipeline, thus leading to a much simplified experimental design. Figure 1 shows how the experimental model pipeline setup relates to the prototype in field conditions.

Proportioning of the model pipeline and polycrystalline ice block sample

Structural integrity must be assured at all times during the operation of a pipeline. In the present context, the effects of internal pressure or the temperature differential were not considered, but these conditions can be accounted for by making use of currently available analytical methods. Flexural strains are induced in the pipeline wall as the pipeline is subjected to increasing differential frost heave movement and thus eventually causing wrinkling (local buckling) in the pipeline. Hence, the design criterion to contain damage due to rupture and leakage of contents is to limit the compressive strain. Two distinct buckling failure modes (Yun and Kyriakides 1990) have been found to occur for buried pipelines. One failure mode is when the pipeline buckles as an overall beam (Euler-type buckling), and usually this mode would be expected when the pipeline is stocky (low ratio of pipeline radius (R) to wall thickness (t)) and very large axial loads are present. The other failure mode is when the principal action is flexural and the resistance is through shell action (thin-walled pipelines), thus enhancing the formation of local wrinkles. It is the latter approach that is more appropriate in the present context. Several criteria have emerged over the years (Southwell 1914; Wilson and Newmark 1933; Bouwkamp and Stephen 1973; Kennedy et al. 1977; Hall and Newmark

1978; Langner 1984; Nyman and Lara 1986; Gresnigt 1986) for limiting flexural strain in tubular pipes. It is not the intent here to provide an exhaustive review of the wrinkling strain criterion, since a brief review has been recently undertaken by Kim and Velasco (1988). The critical strain ε_c is expressed in two general forms:

$$[1] \quad \varepsilon_c = \frac{0.605\,ct}{R}$$

$$[2] \quad \varepsilon_c = \left(\frac{2t}{R}\right)^2$$

where c is a critical strain criterion constant.

The first expression corresponds to the form of a theoretical solution based on elastic buckling developed by Southwell (1914). The second expression stems from a best fit of the experimental data (Sherman 1976; Langner 1984) which distinguishes failures between whether local buckling was observed or not. The constant 0.605 has been determined by Southwell (1914) for elastic buckling, and the constant c was introduced by Wilson and Newmark (1933) to account for experimental deviation. The value of c varies from 1.0 for perfect tubes to 0.25 for manufactured tubes. The lower values of c reflect the importance of initial imperfections present in the geometry of the pipe as shown by Kyriakides et al. (1983). It is also important to note that all criteria based on limiting strain were established from experiments on steel tubes performed in air, i.e., with no restraint from the surrounding medium. The different existing criteria based on experimental tests are summarized in Table 2. Since the critical strain is predominantly a function of the ratio of pipeline radius to wall thickness, the present model pipelines were proportioned so that the model design would be within the range of probable prototype design. The Alaska Gas Pipeline Project envisaged the construction of a 1.22-m-diameter (48 in.) pipeline to transport natural gas from the north slope of Alaska to western Canada for markets in the United States. If pipeline wall thickness of 19 mm (0.75 in.) is assumed, then the R/t ratio for the proposed Alaska Pipeline is about 32. For instance, the pipeline at Caen has a R/t ratio of 28.44. Consequently, for the present experiments two model stainless (seamless) steel pipelines with R/t ratios of 21.43 (19.05 × 0.89 mm) and 20.40 (25.4 × 1.24 mm) were selected. These sizes were readily available in the market and yet

TABLE 2. Summary of critical stain criterion for pipelines

Ref.	Critical strain criteria or constant c	Comments
Southwell (1914)	$c = 1$	Classical elastic solution
Wilson and Newmark (1933); Hall and Newmark (1978)	$c = 0.25$–0.333	Experimentally established; tests performed on 58 tubes (4-in. Shelby tubes and other fabricated specimens)
Bouwkamp and Stephen (1973); Kennedy et al. (1977)	$\varepsilon_c = 0.004$–0.006	Based on 8 tests on large-diameter (48 in.) pipes
Langner (1984); Nyman and Lara (1986)	$c = 0.413$	Over 60 6-in. pipes tested in air and other experimental data
Gresnigt (1986)	$\varepsilon_c = 0.25t/R - 0.0025$	Experimental fit to data from a range of tests

NOTE: $\varepsilon_c = 0.605ct/R$.

of adequate size to permit easy installation of resistance strain gauges on the model pipelines.

An important aspect that needed to be addressed was to suitably dimension the box where the model pipelines were to be embedded in the polycrystalline ice block sample. The length of the box was sized in accordance with the stress-wave length that would be set up along the pipeline. The elastic modulus of polycrystalline ice is dependent on the rate of loading, porosity, salinity and temperature (Michel 1978). It can vary as much as 8 to 10 times less than that of pure ice, as shown by Michel (1978) and Sinha (1989). Sego et al. (1982) demonstrated that the secant elastic modulus for frozen sand is highly dependent on strain rate and that the reduction can be quite large. A range of 40–50 MPa for the elastic modulus of polycrystalline ice was conservatively selected for determining the size of stress wave that would be set up as a result of the prescribed displacement rate. The analysis of a pipeline embedded in a creeping medium (Rajani and Morgenstern 1992) indicated that a pipeline length of approximately 32–40 diameters would be required to represent the semi-infinite length of the pipeline. It is to be noted that the pipeline at Caen had an approximate length/diameter ratio of 33. The width and the height of the box were based on the premise that, when considering the interaction of two adjacent laterally loaded piles, the interaction effects are disregarded if the piles are spaced at least three to four diameters apart. To satisfy this criterion as well as to ensure minimal boundary effects, the box was sized to 0.60 m in width and 0.40 m in height. The box for the sample was manufactured from 18-mm-thick (0.75 in.) PVC sheets. Table 1 compares the principal characteristics of the pipeline at Caen with the model pipelines tested in this study.

Preparation of a polycrystalline ice block sample

The mechanical behaviour of frozen soil has been studied by Sayles (1973), Sayles and Haines (1974), Sego and Morgenstern (1983), and others. It is now widely accepted that ice-rich frozen soil behaves like a creeping material. The frozen soil surrounding the pipeline subjected to frost heave will be associated with primary and secondary creep phases of straining. The classical studies of Glen (1955) indicate that the flow law of polycrystalline ice is that of the Norton type. The Norton creep relationship rewritten in the generalized form as proposed by Ladanyi (1972) is

$$[3] \quad \frac{\dot{\varepsilon}}{\dot{\varepsilon}_0} = \left(\frac{\sigma}{\sigma_0} \right)^n \quad \text{or} \quad \dot{\varepsilon} = B\sigma^n$$

where $\dot{\varepsilon}$ is the axial strain rate; σ is the axial stress; $\dot{\varepsilon}_0$ and σ_0 are proof strain rate and proof stress, respectively; and B and n are the creep constants. Typically, n is about 3 (Morgenstern et al. 1980) for ice or ice-rich silts (McRoberts et al. 1978) subjected to low stresses. In search for a dependence of n and B on temperature, Morgenstern et al. (1980) found from analyses of available creep data that ice behaves close to a linearly viscous material at temperatures close to 0°C. The constant B is found to be dependent on temperature and soil type. In the past, considerable attention has also been paid to the behaviour of polycrystalline ice primarily for glaciology studies and laboratory studies related to geotechnical problems. Sego and Morgenstern (1983, 1985) have studied the behaviour of laboratory-prepared polycrystalline ice and have indeed confirmed the applicability of the Norton-type power law to describe its creep behaviour. Polycrystalline ice is a good material to work with, since control can be exercised over its characteristics (grain size, porosity, etc.) in the laboratory. The decision to use polycrystalline ice in the tests was based on the fact that its elastic and creep properties have been confirmed as result of a considerable amount of testing by different researchers. Another reason for using polycrystalline ice was to reduce the uncertainties in the experimental results so that when it came to comparing theoretical predictions with experimental observations, discrepancies could not be solely attributed to variations in the properties of the surrounding frozen medium.

Details on sample preparation, design of sample box, and construction of the freezing plate are discussed briefly here, but full details can be found in Rajani (1992). The preparation of the block sample required the manufacture of ice that is commonly classified as T1 snow ice. The manufacture of polycrystalline ice has been reported by Sego (1980) and Jacka and Lile (1984). It
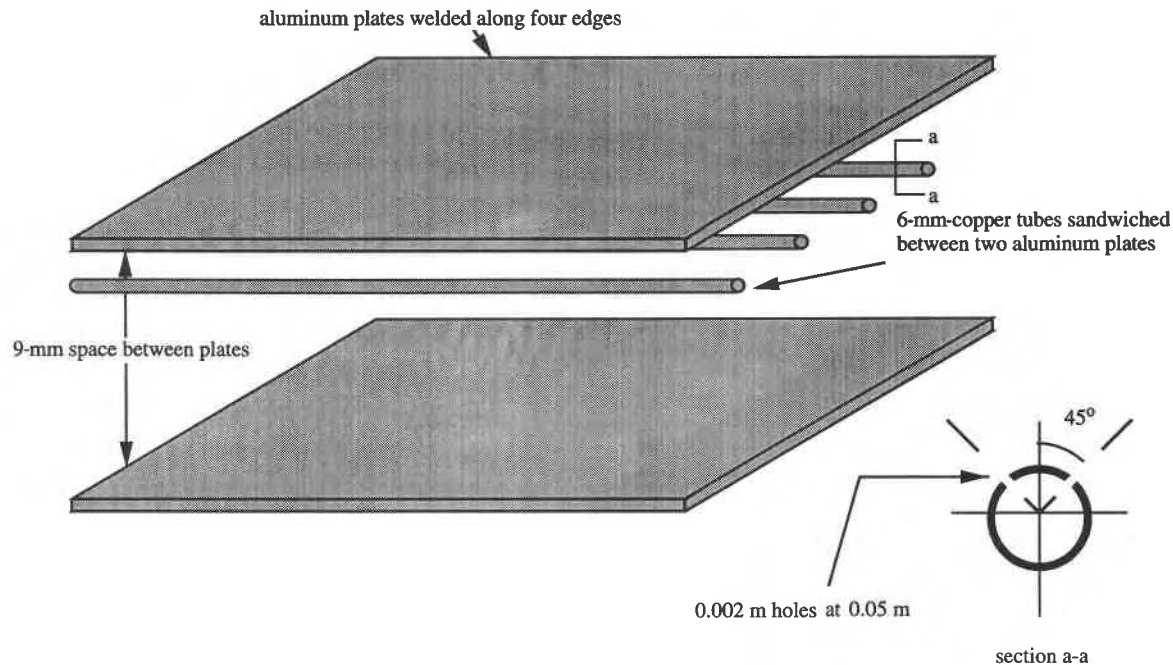
FIG. 2. Exploded view of freezing plate wafer (not to scale).

was desirable to produce snow crystal seeds so that the final ice crystal size in the ice block sample was in the range of 1–2 mm, since properties of polycrystalline ice with this crystal size have been well defined. Sego and Morgenstern (1985) experienced good performance in studies related to experimental indentation of a rigid disk in polycrystalline ice of this type. This meant that the snow crystals had to pass sieve No. 20 and be retained on sieve No. 40, as suggested by Sego (1980). Several methods for obtaining a large quantity of snow with this characteristic were explored and they are discussed fully by Rajani (1992). Thin sections prepared from alternative sources of snow showed no visible differences in polycrystalline ice grain-size distribution. Therefore the decision was made to use natural snow because of abundant availability.

The natural snow crystals were sieved, and those that passed sieve No. 20 but were retained on sieve No. 40 were collected. These presieved snow crystals were rained from a large sieve (No. 20) positioned on top of the box until the box was filled. The application of a vacuum at the top of the box helped draw cold water at near 0°C into the sample through two copper tubes (6.35 mm) with holes placed at the bottom of the sample box above the freezing plate. Normally it took about an hour to saturate the sample with an applied vacuum of 300 mm of mercury. The snow–water slush in the box was frozen unidirectionally as rapidly as possible by feeding liquid nitrogen through the freezing plate (Fig. 2).

Loading arrangement

It was essential to apply a displacement rate at the pipeline end that closely resembled possible field displacement rates as a result of frost heave. At the same time the displacement rate should be slow enough so that strains are in the ductile range of ice deformation The frost heave rate in Caen silt observed at Caen, France, was in the order of 3×10^{-4} mm/min, which is fairly

typical for silty soils. Sego (1980) carried out punch tests on polycrystalline ice at typical penetration rates of $3.83–18.3 \times 10^{-4}$ mm/min. Consequently, a Wykeham Farrance 10-kN capacity press was adapted using a slow motor of 24 min/revolution to obtain a displacement rate of 1.72×10^{-4} mm/min. The loading arrangement is shown in Figs. 3 and 4. The horizontal bars (0.025 × 0.025 m) of the hanger system were not as stiff as initially anticipated for the test on pipeline model A. After completion of the test on pipeline model A, it was observed that the bars had undergone permanent plastic deformation. A calibration test was carried out on the hanger system, and it was found that the displacement rate at the pulling end of the pipeline was about one-third of that measured at the platen of the Wykeham Farrance machine. This reduced displacement rate was used for the finite element analysis discussed later. As a consequence, much stiffer horizontal bars (0.025 × 0.050 m) were used for pipeline model B with the intention of reducing the compliance in the loading hanger.

Instrumentation

The model pipelines were instrumented with resistance strain gauges along the length of the pipeline. Strain gauges were located at both top and bottom for the first model pipeline (19.05 × 0.89 mm), and a full wheatstone bridge was established between them so as to avoid problems with temperature compensation. Though this approach permitted the use of a reduced number of strain gauges, it was recognized that the true local strain in the pipeline would be difficult to ascertain. Consequently, independent top and bottom strain gauges were used for model pipeline B (25.4 × 1.24 mm) to remove any possible uncertainty. The strain gauges on the model pipeline A were protected by wrapping the pipe with a heatshrink teflon-type material (FIT 221 produced by Alfa Wire Corporation). The teflon material was also chosen to represent some sort of field coating. Since an adequate
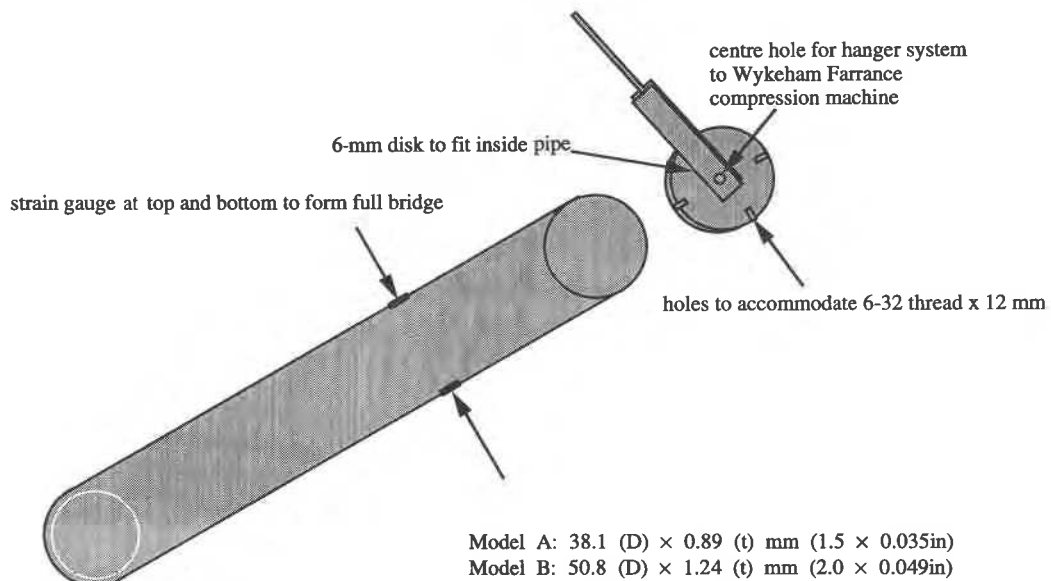
FIG. 3. Typical strain gauge arrangement and hanger system for applying displacements.
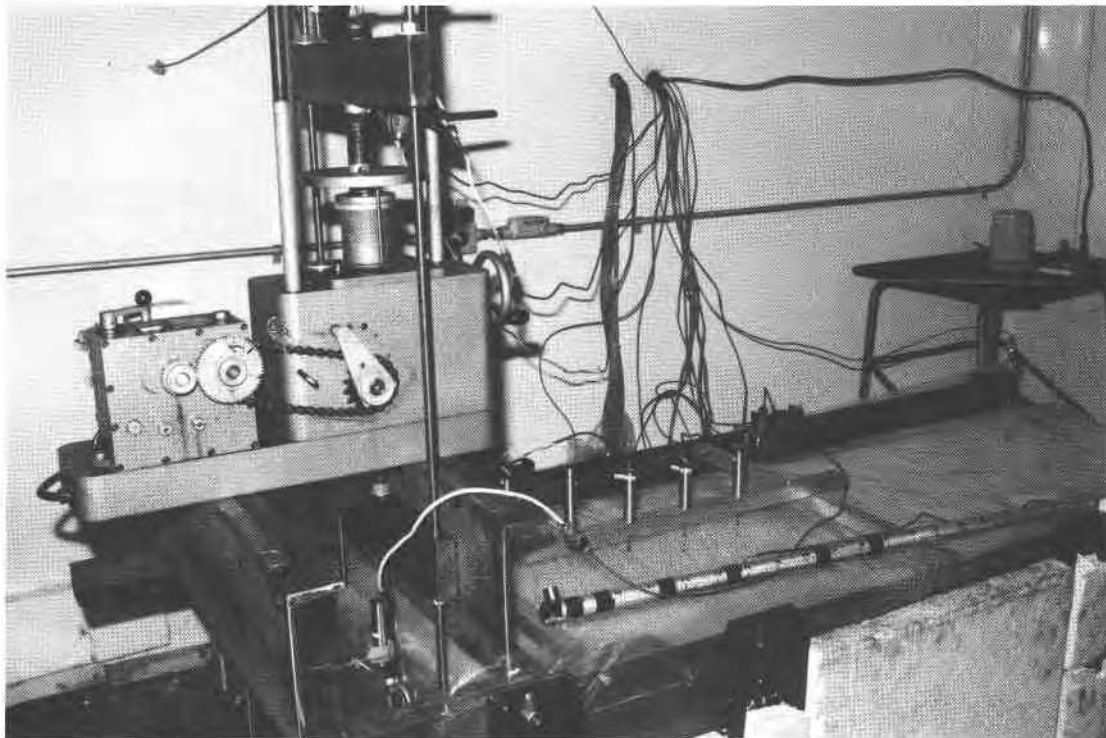

FIG. 4. General loading arrangement of an embedded model pipeline.

size of heat shrink was not available for the model pipeline B, a different wrapping material (Nitto Butyl 2-in. self-vulcanization rubber tape) was used. The model pipelines were calibrated prior to testing under a cantilever loading arrangement. In addition, the movement of the platen of the compression machine and the corresponding force imposed on the pipeline were monitored by a linear voltage displacement transducer (LVDT) and a load cell, respectively. The displacements along the pipeline close to the loaded end were monitored using closely spaced LVDTs. The LVDTs were placed at the crest of the pipes through holes drilled in the ice block

sample A. An alternative procedure was used for pipeline model B where thin tubular stems were attached to the crest of the pipeline prior to freezing. These tubes acted as guides for free movement of the LVDT rods. The Hewlett Packard 24 LVDTs are capable of measuring displacements to an accuracy of 0.0012 mm. All the data were logged automatically every 2 h by a PC for easy retrieval using an electronic spreadsheet.

Elastic and creep properties of polycrystalline ice

It is to be expected that polycrystalline ice surrounding the model pipeline will be subjected to tensile stresses as
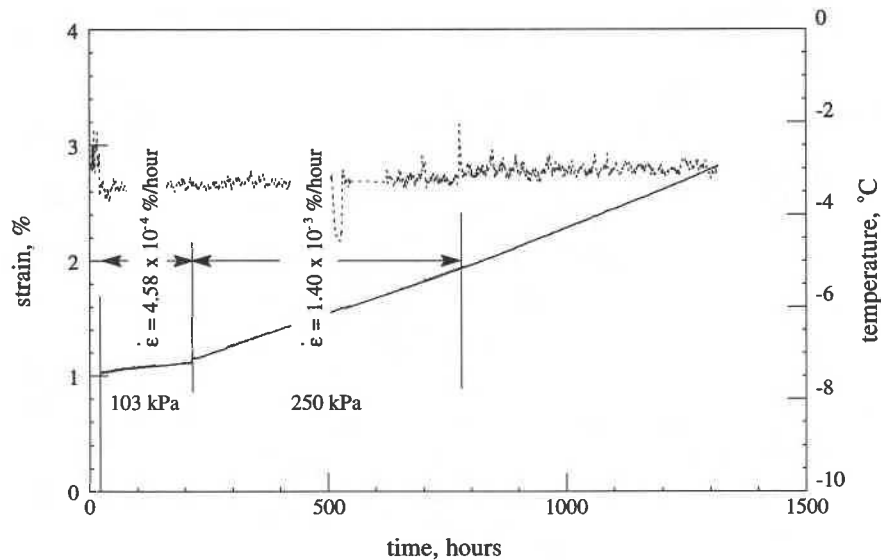
FIG. 5. Constant-load creep test for polycrystalline ice sample T1-10/91.

the pipeline is displaced upward. However, good tensile creep tests are difficult to perform, and only limited data are presently available. Zhu and Carbee (1987) carried out both compressive and tensile creep tests on ice-rich silt from Fairbanks, Alaska. Their purpose was to determine the influence of applied stress (or applied strain rate) and temperature on strength and creep behaviour of frozen silt. Zhu and Carbee found that if the strain rate was below 10^{-2}/s then there was essentially no difference in the tensile or compressive behaviour of frozen silt. Recent experimental work on tensile behaviour of frozen soils (silt, sand, and gravel) by Sayles (1991) confirms the findings of Zhu and Carbee (1987). Hawkes and Mellor (1972) also reported that there was no difference in tensile and compressive creep behaviour in polycrystalline ice for strain rates less than 10^{-6}/s.

The model pipeline tests were displaced at strain rates of $6-8 \times 10^{-8}$/s (the displacement rates were normalized by the diameter of the pipeline). Compressive and not tensile creep testing on polycrystalline ice was conducted because of the fact that the strain rates were anticipated to be less than 10^{-6}/s and considering the fact that adequate equipment required to perform tensile tests was not readily available. It is to be emphasized that the creep tests were conducted only to reassure that a large sample of polycrystalline ice with the desired and known characteristics had been prepared.

Intact core samples of 0.10 m (diameter) × 0.3 m (height) were taken from the ice sample blocks where the pipeline models were tested using a CRREL coring barrel. Thin sections obtained from typical samples examined under polarized light showed near uniformity of crystal size, and the background grid (10 × 10 mm) permitted a rough estimate of the size of the individual crystals. The thin sections were obtained by the hot-plate method as described by Sego (1980). The sonic elastic properties were obtained using piezoelectric crystals that detected the arrival of P- and S-waves. The testing procedure used is given in detail by A. Instanes.[2] Typical

value for dynamic elastic moduli were within the 3–7 GPa range. Typical constant-load tests were carried out on 0.10-m (4 in.) samples (typically height to diameter ratio was 2) at different loads. The procedure for the constant-load creep test was essentially as outlined by Sego (1980), except that a multistaged loading procedure was applied on most samples. Typical axial strain – time history for one of the samples is shown in Fig. 5. The strain histories indicate that at low stresses (i.e., <210 kPa) primary creep had terminated after about 100–150 h. The experimental results of the creep multistaged constant-load tests are summarized in Table 3. The strain rates were corrected only for temperature as suggested by Sego (1980). A grain-size correction was not deemed necessary, since the ice crystals in present samples were within the 1-mm range and the fact that Sego's (1980) data are normalized with respect to a crystal size of 1 mm. The corrected normalized displacement rates are shown in Fig. 6 together with data from Sego (1980) and others. Morgenstern et al. (1980) have thoroughly reviewed available data on creep properties of ice, and they have determined the influence of temperature. The creep test results from the present series of tests on polycrystalline ice were analyzed together with other relevant data shown in Fig. 6, and the creep constants B and n were obtained. Table 4 shows these creep properties together with those obtained by Morgenstern et al. (1980). The data from tests on polycrystalline ice reported here serve to confirm that the creep properties of the ice block samples prepared for testing the model pipelines are within the expected range. The creep properties (corrected for temperature) established by Morgenstern et al. (1980) were used in the finite element analyses for predicting strains in the pipeline since these properties were based on an exhaustive review of the data on polycrystalline ice available then.

Structural properties of pipeline steel 304

A 0.3-m-long section from each of the model pipelines was instrumented with strain gauges to determine the structural properties of stainless steel 304. Custom-made stems were welded to both ends of the test specimen so

[2]"Sonic and mechanical properties of spray ice," Ph.D. thesis, University of Trondheim, Norway. In preparation.

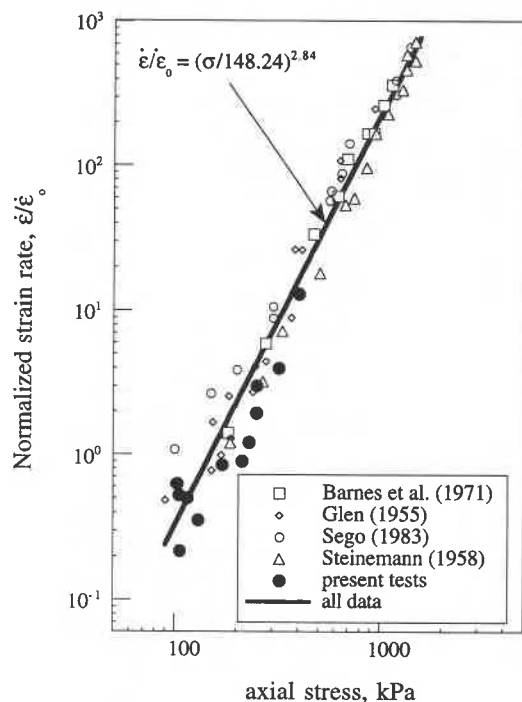$$\dot{\epsilon}/\dot{\epsilon}_0 = (\sigma/148.24)^{2.84}$$

FIG. 6. Corrected normalized strain rate vs. axial stress for polycrystalline ice at $-2°C$.
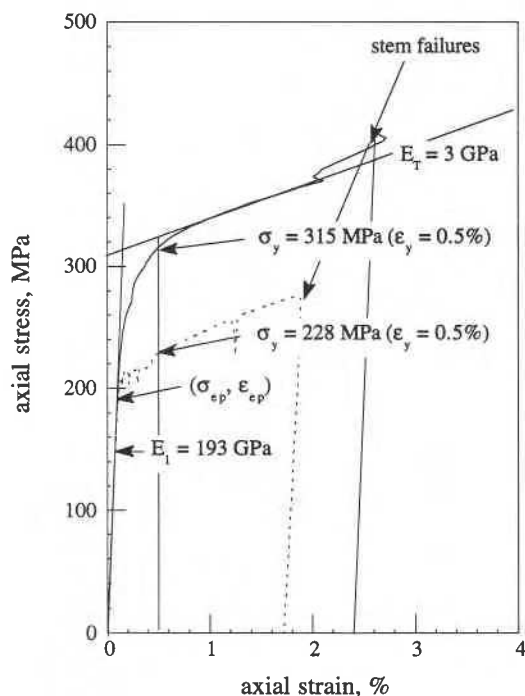

FIG. 7. Experimental stress–strain characteristics of pipeline models A (—) and B (- - -) (stainless steel 304). $\sigma_{ep} = 193$ MPa; $\epsilon_{ep} = 0.1\%$.

TABLE 3. Summary of constant-load creep test on samples of polycrystalline ice

Sample	Density (Mg/m^3)	Temperature[a] (°C)	Stress (kPa)	Corrected strain rate
T1-10/91	0.876	−2.7(1.20)	115	0.495
		−3.0(1.28)	213	0.882
		−3.0(1.28)	230	1.193
		−2.0(1.00)	130	0.351
T2-11/91	0.864	−4.3(1.61)	400	12.98
A4-01/92	0.862	−5.0(1.77)	106	0.216
		−5.0(1.77)	250	2.977
		−3.2(1.33)	320	3.945
B5-01/92	0.848	−3.4(1.38)	105	0.519
		−4.0(1.54)	170	0.843
B7-02/92	0.853	−3.3(1.36)	103	0.622
		−3.3(1.36)	250	1.903

[a]The values in parentheses are correction factors for strain rates normalization at $-2°C$.

TABLE 4. Creep properties of polycrystalline ice at $-2°C$

Ref.	Creep exponent n	Creep coefficient B (kPa^{-n}·year^{-1})
Morgenstern et al. (1980)	3.00	2.03×10^{-8}
Present creep tests and others reported by Sego (1980)	2.84	5.98×10^{-8}
Parameters used for analysis ($-3°C$)	3.00	1.53×10^{-8}

Canadian Standards Association (1979) is in the 228–315 MPa range at a strain of 0.5% (ϵ_y). Stainless steel 304 maintains stress–strain elastic proportionality (ϵ_{ep}) until 0.1% axial strain. It is interesting to note that a much lower yield strength was attained by the pipeline model B.

Observation of strain–time histories in model pipelines

Data for only one of the tests are discussed here although two model pipelines described earlier were tested. The overall behaviour of the two model pipelines was observed to be similar and complete data on both tests can be found in Rajani (1992). The displacement–time and load–time histories monitored at the free end of the pipeline model A are shown in Fig. 8. While pipeline A was being steadily displaced, the end load increased for about 1000 h when it stabilized at a load level of 2744 N. During the test on pipeline model A, the monitoring of the ice temperature (Fig. 9) commenced after problems were detected in the refrigeration system. The temperature was monitored by setting a thermistor (resistance temperature detector) in the ice block sample at a depth of 0.10 m. A gap was noted to develop at the back of the pipeline as it was steadily displaced upwards. The flexural strain – time history for pipeline model A is shown in Fig. 10.

The deformed shape of the pipeline obtained from the LVDTs placed at the crest of the pipeline is shown in Fig. 11. The deformed shape measured after the comple-

that specimens could be tested in the available MTS testing machine. The loading speed was slightly increased at about 2% strain for the first specimen, and the tests were prematurely terminated when a weld failure occurred at the stem–specimen connection. The structural steel characteristics determined from the tests (Fig. 7) are summarized in Table 1. The yield stress (σ_y) as defined by the
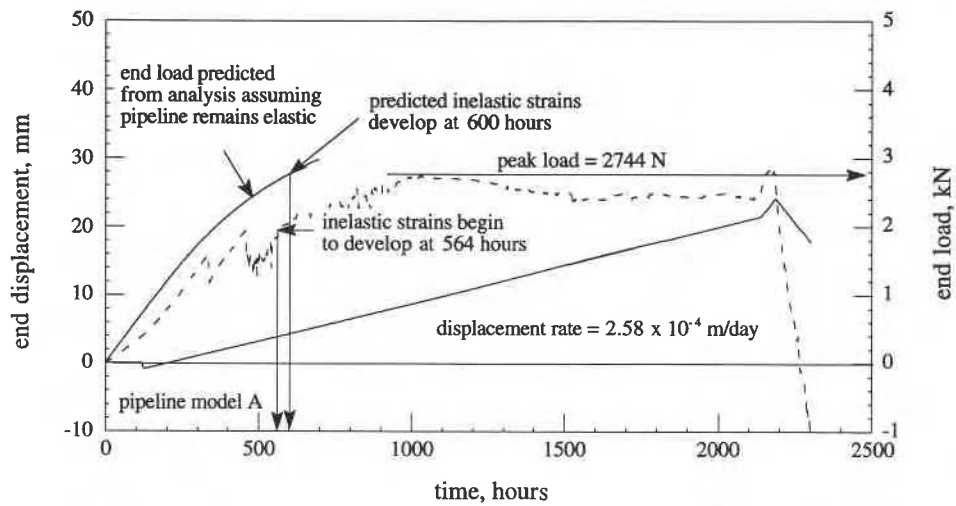
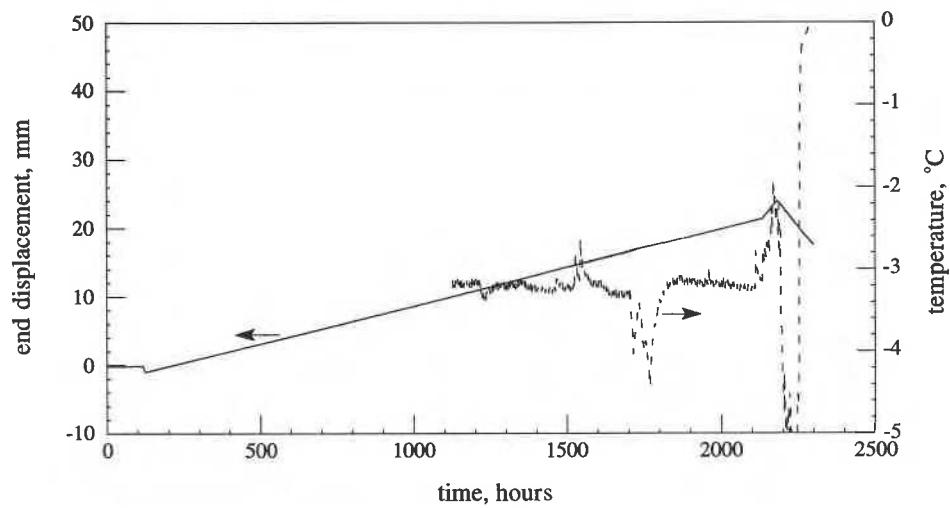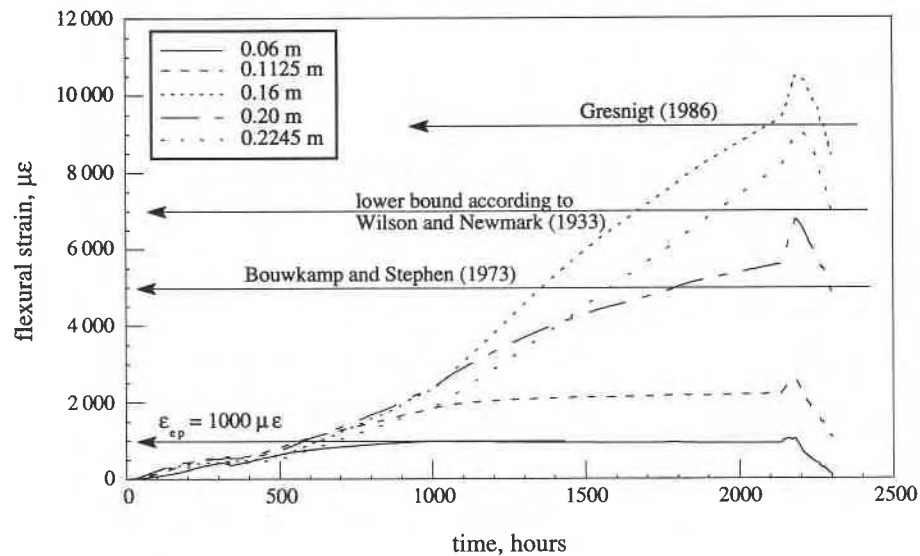FIG. 8. End displacement and load–time histories for pipeline model A.

FIG. 9. End displacement – time and temperature–time histories for pipeline model A. Displacement rate = 2.58 × 10⁻⁴ m/day.

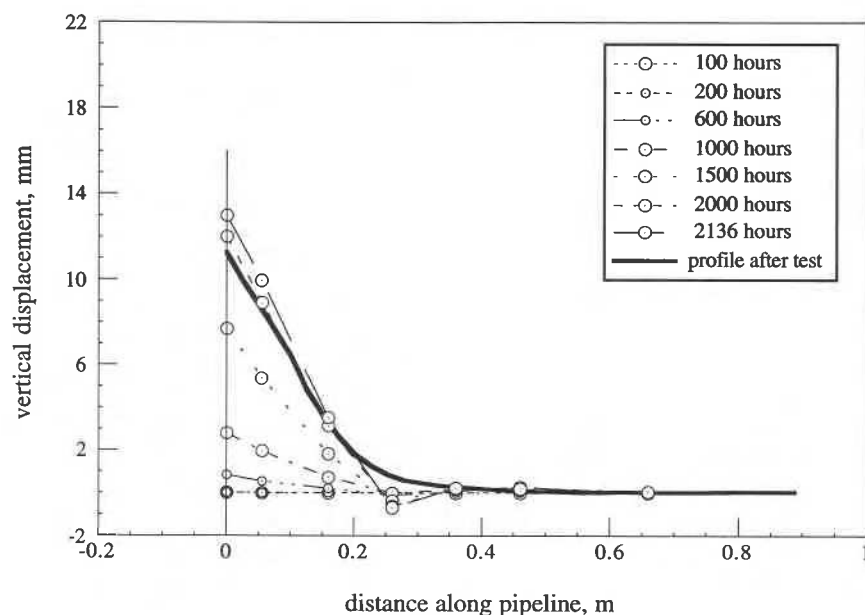FIG. 10. Strain–time histories for points in the immediate vicinity of the peak strains for pipeline model A.

FIG. 11. Vertical displacement profile histories for pipeline model A. Stainless steel 304 pipeline, 38.91 mm (1.5 in.) diameter × 0.889 mm (0.035 in.) wall thickness.
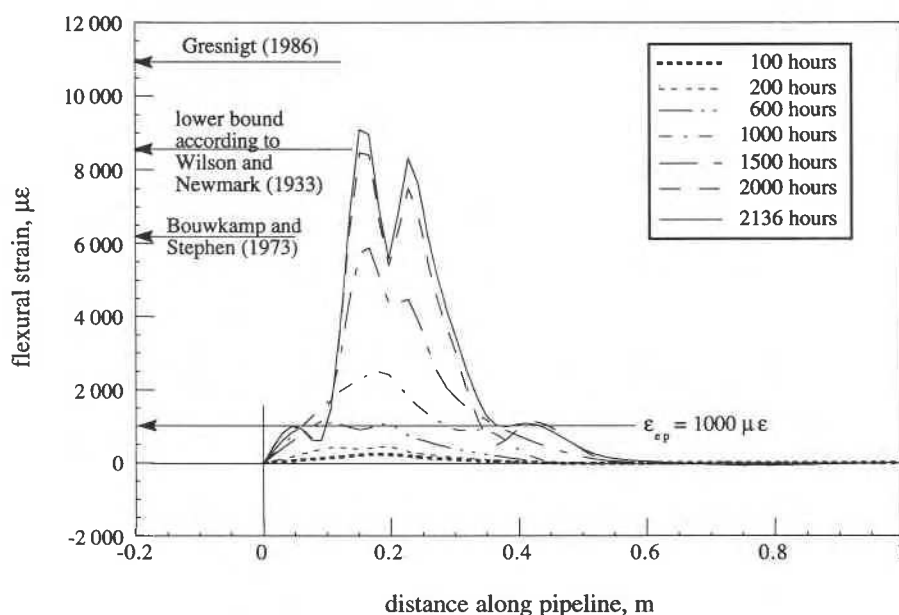

FIG. 12. Experimental flexural strain profile histories for pipeline model A.

tion of the test (pipeline model A) compared well with the last monitored shape and provided additional evidence on the reliability of the LVDTs during the test that lasted for about 90 days.

The flexural-strain profiles developed along the pipeline model A for different time intervals are shown in Fig. 12. The stress imposed on the ice as a result of the load developed at the end of the pipe (pulling end) can be estimated approximately from statics if a fully plastic moment is assumed to develop at the point of maximum strain. This approach gives an estimate of the average resistance due to uplift of the pipeline. The average reaction intensity calculated in this manner for pipeline model A is within the 100–300 kPa range. As noted

before, the constant-load creep data on polycrystalline ice indicate that primary creep is over after about 150 h, and consequently the application of Norton's secondary creep flow law for analysis is satisfactory for practical purposes. The strain profile is observed to be fairly smooth for the first 600 h approximately for pipeline models A and B when the strains are below 0.1%. Thereafter the material of the pipeline model response is nonlinear. After the tests were completed, the deformed profile of the bent pipeline models was obtained along the crest of the pipeline at 25-mm intervals. The final curvature was then estimated from the deformed shape using a three-point finite-difference formula. Since the determination of the curvature essentially involves
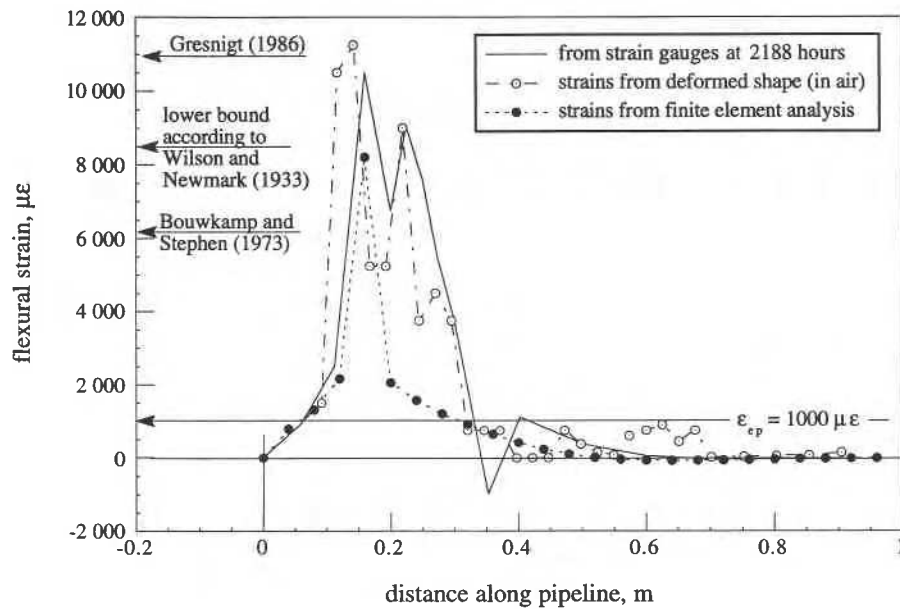
FIG. 13. Comparison of final flexural strain profile time histories before thaw obtained from strain gauges, strains determined from deformed shape, and predicted strains for pipeline model A.

numerical differentiation, the results can be very sensitive to small variations in the original data. However, the purpose of determining the flexural strains from the permanent deformed shape of pipeline models was only to confirm the final strains measured using electrical resistance strain gauges. A more elaborate procedure, such as fitting a cubic spline or a high-order polynomial to the deformed shape, was not attempted for the same reasons stated earlier. The flexural strains were estimated from curvatures, assuming that the neutral axis was still at the centre of the pipe. A comparison of the peak strains (Fig. 13) obtained from the two different methods indeed confirmed that the electrical resistance strain gauges had performed satisfactorily throughout the tests.

Circumferential measurements at different sections along the model pipelines were obtained to determine if significant ovality of the circular cross section had taken place. Figure 14 shows the deformed cross-sectional shape (exaggerated 20 times) of the pipeline at different sections of the pipeline. The circumferential readings were performed with a displacement dial gauge with an accuracy of 0.0254 mm (0.001 in.). These measurements were also confirmed independently using an electronic caliper. The maximum ovality δ (inward) registered is in the order of 0.15 mm. In terms of the net diametrical change $d_i(\%) = 2(\delta/D)100$, this amounts to a change of 0.78%. In fact the ovality is hardly discernible, and no wrinkles or substantial local deformations were present.

Discussion of experimental results

If pipeline models A and B were to represent the prototype, then it is most probable that the pigging serviceability of these pipeline models would not be affected. Serviceability is not hindered despite the fact that all strain limits, as suggested by Wilson and Newmark (1933), Bouwkamp and Stephen (1973), Sherman (1976), and Gresnigt (1986), were exceeded (Fig. 13). It is most probable that the restraint offered by the surrounding stiff medium arrests the formation of wrinkles, and sub-
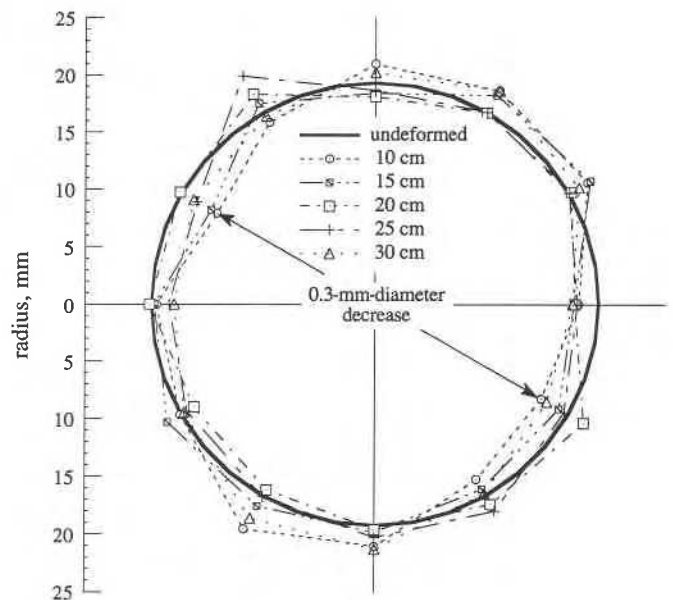

FIG. 14. Out-of-roundness profiles at different sections along pipeline model A.

stantially more flexural strain, as a result of frost heave, can be tolerated before serviceability would be severely hindered. Yun and Kyriakides (1990) found through analysis of shell buckling that imperfections have a dominant effect over the restraint offered by a stiff medium for the load-carrying capacity for a pipeline subjected to axial loads. Even though the restraint offered by the surrounding stiff medium does not affect the load-carrying capacity, it has a notable effect on the critical strain. It is important to make this distinction because design criteria are based on serviceability with respect to pigging as well as the need to avoid rupture when subjected to uplift due to frost heave. A similar situation (Yudovich and Morgan 1989) arises for deep oil–gas casings where
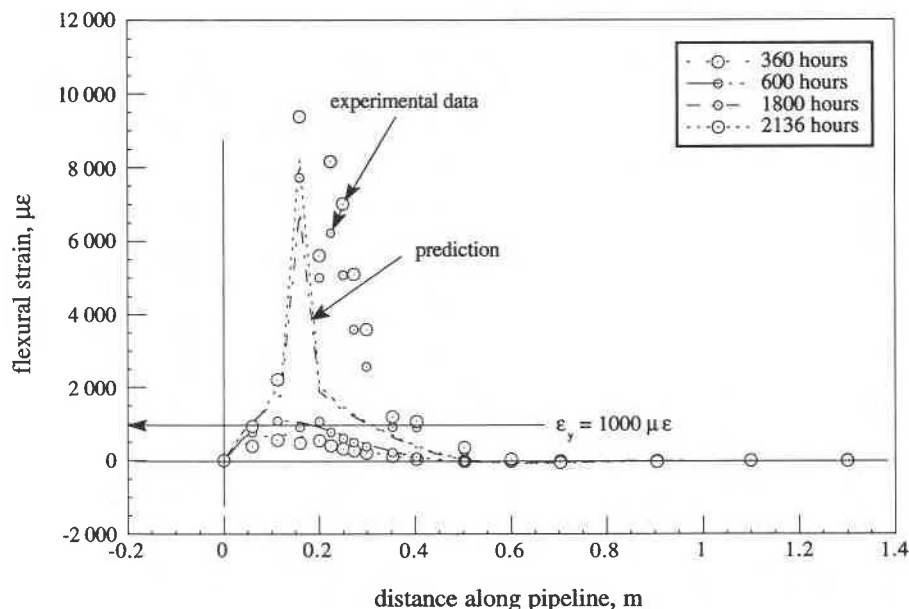
Fig. 15. Comparison of measured and predicted flexural strain profiles for pipeline model A.

loading on the casings is imposed by the collapse of high-porosity chalks in reservoirs at the Ekofisk site in the North Sea. Since these reservoirs are deep, the stiffness of the surrounding chalk would be high because its elastic modulus is dependent on the confining stress. Statistical analyses of casing serviceability and critical strain indicated that strains as high as 5–6% could be tolerated without posing a major hindrance for casing service.

Comparison of experimental behaviour with analysis

The numerical Winkler model developed for a beam embedded in a creeping medium (Rajani and Morgenstern 1992) was used to evaluate the response of the model pipelines subjected to steady displacement for over 2000 h. The finite element analyses were performed using Adina R&D, Inc. (1984), where the polycrystalline ice is represented by discrete creeping springs and the pipeline itself is represented by beam elements. Adina R&D, Inc. (1984) permits the specification of a tubular cross section whereby the material nonlinearity can be taken into account in the simplest form. The material nonlinearity of steel was limited to a bilinear relationship along the lines suggested by the Committee on Gas and Liquid Fuel Lifelines (1984). All the pertinent data for individual components of the pipeline – polycrystalline ice which were discussed earlier helped to define all the relevant properties with minimal uncertainties.

The strain-wave profile during the initial period, i.e., before 512 h, helped to establish the elastic subgrade foundation modulus (i.e., elastic modulus of the surrounding ice). Since the solution for a beam embedded in a creeping medium is based on the correspondence principle, it is essential to match the elastic response with the form of the initial observed response. The procedure used was essentially the same as that discussed by Rajani and Morgenstern (1992). Identification of the location of the peak strain permitted the determination of the most appropriate value of elastic or instantaneous modulus of ice, which was estimated to be 61 MPa for

both models A and B. The marked difference between the elastic modulus determined from sonic measurements and from pipeline–ice interaction is related to strain-rate effects. Another source of discrepancy is perhaps in the limitation of Biot's (1937) or Vesic's (1961) formulae to translate the elastic continuum properties to foundation subgrade modulus. In the nonlinear analysis an integration order of $5 \times 3 \times 5$ (r, s, θ) was used for the pipe beam element. Tawfik (1986) argues that the trilinear material model as proposed by the Committee on Gas and Liquid Fuel Lifelines (1984) for steel can lead to considerably higher estimated strains than would be obtained by a curvilinear material model like the Ramberg-Osgood model. This is primarily due to the fact that at large strains (>4%) no stiffness is attributed to the material. This effect need not be of concern in the present analysis, since the strains do not approach this strain limit. Nonetheless, Tawfik (1986) observes that when the material model is represented by the curvilinear form, the strain wave is of an oscillatory nature near zones where plastic deformations take place. A bilinear stress–strain relation for steel was selected for the finite element nonlinear analysis, and the prediction of peak strain was largely dependent on the elastic limit established from the uniaxial tests discussed earlier. If a bilinear stress–strain relation as suggested by the Committee on Gas and Liquid Fuel Lifelines (1984) is used, then the predicted peak strains are considerably reduced. This observation also confirms Tawfik's (1986) findings that a discontinuous representation of the stress–strain relation for steel is not quite appropriate for realistic predictions.

Figure 15 shows the comparison of predicted and measured strain profiles at different time periods. The predicted and experimental flexural strain profiles match quite well for strains below the elastic strain proportionality limit (ε_{ep}) of 1000 $\mu\varepsilon$. However, for strains beyond the elastic strain proportionality limit, the extent of predicted plastic deformations (predicted versus measured) also compares well except that the predicted peak flexural strains are considerably higher than those

observed. The principal reason for this discrepancy is due to the fact that the pipeline is represented by a two-dimensional beam element in the finite element analyses and, since the discretization is too coarse (typically one diameter of pipe), it is unable to account for stress redistribution that takes place in the pipeline as significant plastic strains develop. However, a three-dimensional analysis, where the pipe is represented by shell elements and surrounding medium by three-dimensional brick elements, would perhaps reproduce this redistribution of stresses more realistically, but the analysis would be prohibitively costly.

Conclusions

A thorough description of the experimental procedure for carrying out model pipeline tests has been provided. Two different model size pipelines were tested in polycrystalline ice with continuous monitoring of flexural strains, displacements, and temperature. Evidence from the Caen experimental facility and the analysis of a beam embedded in a creeping medium studied by Rajani and Morgenstern (1992) indicate that a half-sinusoidal stress or strain wave is set up along the pipeline as the pipeline steadily displaces upward at one end. The experimental data from the model pipelines indeed confirm that a half-sinusoidal strain wave is formed along the pipeline and a redistribution of stresses takes place once some portion of the model exceeds the yield stress. It seems that, though the burial of the pipeline is shallow, for the purpose of this analysis it can be regarded as being deeply buried if the surrounding medium is very stiff.

Although the R/t ratio of the model pipelines is on the low side in comparison to a prototype pipeline, buckling or wrinkling was not observed as in the experiments conducted by Bouwkamp and Stephen (1973) or Stephens et al. (1982). Although there is undoubtedly loss of contact at the bottom of the pipe displaced upward, inward ovalization at the crown would be accompanied by outward bulging at the quarter points where stiff restraint from the ice would be encountered. Nonetheless, it is to be noted that out-of-roundness measurements did not indicate any significant ovalization. This mechanism of restraint offered by the surrounding media has been discussed by Gresnigt (1986) and provides evidence that it is an important mechanism to consider for pipeline – frozen soil interaction. Though the strains exceeded currently accepted strain limits, the serviceability was not hindered. We therefore infer that the surrounding stiff medium retards the formation of wrinkles. This suggests that the critical strain limit can be increased considerably without jeopardizing the reliability of the pipeline. The experimental results presented in this paper do indicate that more tests are required to confirm the findings of this paper, and pipelines with higher R/t and scaling ratios should be tested.

Adina R&D, Inc. 1984. A finite element program for automatic dynamic incremental nonlinear analysis. Adina R&D, Inc., Boston. Report AE 84-1.

American Society of Civil Engineers. 1978. An overview of the Alaska highway gas pipeline: the world's largest project. National Convention of the American Society of Civil Engineers, Pittsburgh, Penn.

Biot, M.A. 1937. Bending of an infinite beam on an elastic foundation. Transactions, ASCE Journal of Applied Mechanics, **59**: A1–A7.

Bouwkamp, J.G., and Stephen, R.M. 1973. Large diameter pipes under combined loading. ASCE Transportation Engineering Journal, **99**(TE3): 521–536.

Canadian Standards Association 1979. Steel Line Pipe. Canadian Standards Association, Rexdale, Ont. Report CAN/CSA-Z245.1.

Committee on Gas and Liquid Fuel Lifelines. 1984. Guidelines for the seismic design of oil and gas pipeline systems. American Society of Civil Engineers, New York.

Dallimore, S.R., and Crawford, H. 1985. Experimental observations of differential heaving and thaw settlement around a chilled pipeline. *In* Pipelines and frost heave. Proceedings of a Seminar held at Centre de géomorphologie, Caen, France. *Edited by* S.R. Dallimore and P.J. Williams, Carleton University, Ottawa. pp. 5–17.

Foriero, A., and Ladanyi, B. 1991. Generalized finite-element algorithm for laterally loaded piles in permafrost in comparison with measurements. Canadian Geotechnical Journal, **28**: 523–541.

Geotechnical Science Laboratories. 1986. Investigations of frost heave as a cause of pipeline deformation. Carleton University, Ottawa. Report IR-50.

Geotechnical Science Laboratories. 1988. The third freeze cycle of the Canada–France ground freezing experiment. Carleton University, Ottawa. Report IR-54.

Geotechnical Science Laboratories. 1989. Canada–France pipeline – ground freezing experiment. Carleton University, Ottawa. Report IR-58.

Glen, J.W. 1955. The flow law of polycrystalline ice. Proceedings of the Royal Society of London, Series A, **228**: 519–538.

Gresnigt, A.M. 1986. Plastic design of buried steel pipelines in settlement areas. Heron, **31**(4): 1–113.

Hall, W.J., and Newmark, N.M. 1978. Seismic design criteria for pipelines and facilities. ASCE Journal of Technical Councils, **104**(TC1): 91–107.

Hawkes, I., and Mellor, M. 1972. Deformation and fracture of ice under uniaxial stress. Journal of Glaciology, **11**(61): 103–131.

Jacka, T.H., and Lile, R.C. 1984. Sample preparation techniques and compression apparatus for ice flow studies. Cold Regions Science and Technology, **8**(3): 235–240.

Kennedy, R.P., Chow, A.W., and Williamson, R.A. 1977. Fault movement effects on buried pipelines. ASCE Transportation Engineering Journal, **103**(TE5): 617–633.

Kim, H.O., and Velasco, P. 1988. Review of pipe buckling for arctic pipeline design. Proceedings, 7th International Conference on Offshore Mechanics and Arctic Engineering, Houston, Tex. *Edited by* J.S. Chung. American Society of Mechanical Engineers, New York. Vol. 5. pp. 307–315.

Kyriakides, S., Yun, H.D., and Yew, C.H. 1983. Buckling of buried pipelines due to large ground movements. *In* Earthquake behaviour and safety of oil and gas storage facilities, buried pipelines and equipment. *Edited by* T. Ariman. American Society of Mechanical Engineers, New York. Publication PVP 77. pp. 140–150.

Ladanyi, B. 1972. An engineering theory of creep of frozen soils. Canadian Geotechnical Journal, **9**: 63–80.

Langner, C.G. 1984. Design of deepwater pipelines. Proceedings, TNO-IWECO 30th Symposium on Underwater Technology, The Hague, Netherlands.

McRoberts, E.C., Law, T.C., and Murray, T.K. 1978. Creep tests on undisturbed ice-rich silt. Proceedings, 3rd International Permafrost Conference, Edmonton, Alta., Vol. 1. pp. 539–545.

Michel, B. 1978. Ice mechanics. Les Presses de l'Université de Laval, Québec.

Morgenstern, N.R., Roggensack, W.D., and Weaver, J.S. 1980. The behaviour of friction piles in ice and ice-rich soils. Canadian Geotechnical Journal, **17**: 405–415.

Nixon, J.F. 1984. Laterally loaded piles in permafrost. Canadian Geotechnical Journal, **21**: 431–438.

Nixon, J.F., Morgenstern, N.R., and Ressor, S.N. 1983. Frost heave – pipeline interaction using continuum mechanics. Canadian Geotechnical Journal, **20**: 251–261.

Nyman, K.J., and Lara, P.F. 1986. Structural monitoring helps assess deformations in arctic pipelines. Oil and Gas Journal, **81**(11): 81–86.

Rajani, B. 1992. Deformation of pipelines embedded in frozen soil. Ph.D. thesis, University of Alberta, Edmonton.

Rajani, B., and Morgenstern, N. 1992. Behaviour of a semi-infinite beam in a creeping medium. Canadian Geotechnical Journal, **29**: 779–788.

Sayles, F.H. 1973. Triaxial and creep tests on Ottawa sand. Proceedings, 2nd International Conference on Permafrost, Yakutsk, North American Contribution. pp. 384–391.

Sayles, F.H. 1991. Stress–strain behaviour of frozen soil in tension. Proceedings of Canada–France Seminar: Gas pipelines, oil pipelines, civil engineering in Arctic climates, Caen, France. *Edited by* P.J. Williams. pp. 61–72.

Sayles, F.H. and Haines, D. 1974. Creep of frozen silt and clay. U.S. Army Corps of Engineers, Cold Regions Research and Engineering Laboratory, Hanover, N.H. Technical Report 252.

Sego, D.C. 1980. Deformation of ice under low stresses. Ph.D. thesis, University of Alberta, Edmonton.

Sego, D.C., and Morgenstern, N. 1983. Deformation of ice under low stresses. Canadian Geotechnical Journal, **20**: 587–602.

Sego, D.C., and Morgenstern, N. 1985. Punch indentation of polycrystalline ice. Canadian Geotechnical Journal, **22**: 226–233.

Sego, D.C., Shultz, T., and Banasch, R. 1982. Strength and deformation behaviour of frozen saline sand. Proceedings, 3rd International Symposium on Ground Freezing, Cold Regions Research and Engineering Laboratory, Hanover, N.H. pp. 11–17.

Sherman, D.R. 1976. Tests of circular steel tubes in bending. ASCE Journal of the Structural Division, **102**(ST11): 2181–2195.

Sinha, N.K. 1989. Elasticity of natural types of polycrystalline ice. Cold Regions Science and Technology, **17**(2): 127–135.

Southwell, R.V. 1914. On the theory of elastic stability. Philosophical Transactions of the Royal Society of London, Series A, **213**: 187–244.

Stephens, M.J., Kulak, G.L., and Montgomery, C.J. 1982. Local buckling of thin-walled tubular members. University of Alberta, Structural Engineering Report 103.

Tawfik, M.S. 1986. Analysis of pipelines under large soil deformations. Ph.D. thesis, Cornell University, Ithaca, N.Y.

Vesic, A.S. 1961. Bending of beams resting on isotropic elastic solid. ASCE Journal of the Engineering Mechanics Division, **87**(EM2): 35–51.

Wilson, W.M., and Newmark, N.M. 1933. The strength of thin cylindrical shells as columns. University of Illinois, Experimental Station, Urbana. Bulletin 255.

Yudovich, A., and Morgan, D.R. 1989. Casing deformations in Ekofisk. Journal of Petroleum Technology, **41**(7): 729–734.

Yun, H., and Kyriakides, S. 1990. On the beam and shell modes of buckling of buried pipelines. Soil Dynamics and Earthquake Engineering, **9**(4): 179–193.

Zhu, Y., and Carbee, D.L. 1987. Tensile strength of frozen silt. U.S. Army Corps of Engineers, Cold Regions Research and Engineering Laboratory, Hanover, N.H. Report 87-15.

Nomenclature

B	creep proportionality constant
c	critical strain criterion constant
D	pipeline diameter $(= 2R)$
E_1	beam elastic modulus
E_T	steel strain hardening modulus
E_s	soil elastic modulus
h	embedment depth
n	creep exponent in Norton relation
R	radius of model pipelines
t	pipeline wall thickness
ε_c	critical strain
$\dot{\varepsilon}$	axial strain rate
$\dot{\varepsilon}_o$	proof strain rate
ε_{ep}	elastic proportionality strain limit
γ	soil weight density
ν	steel Poisson's ratio
ν_s	soil Poisson's ratio
σ_{ep}	elastic proportionality stress limit
σ_y	steel yield stress
σ_o	proof stress
σ	axial stress
ε_y	yield strain
d_i	net diametrical change
δ	ovality
r, s, θ	radial, axial, and circumferential axes for pipe beam element
e	void ratio